XI International Conference on Computational Plasticity. Fundamentals and Applications
COMPLAS XI
E. Oñate, D.R.J. Owen, D. Peric and B. Suárez (Eds)

HIGH TEMPERATURE EFFECTS IN MORTAR AND CONCRETE SPECIMENS USING A MESO-MECHANICAL MODEL WITH FRACTURE BASED ZERO-THICKNESS INTERFACE ELEMENTS

M. RODRÍGUEZ[1], C.M. LÓPEZ[1], I. CAROL[1], J. MURCIA[2]

[1] Department of Geotechnical Engineering and Geo-Sciences
ETSECCPB (School of Civil Engineering)-UPC (Technical Univ. of Catalonia), 08034 Barcelona
[2]Instituto Eduardo Torroja CSIC, 28033 Madrid, Spain.
E-mail: carlos.maria.lopez@upc.edu, ignacio.carol@upc.edu

Key words: High temperature effects in mortar and concrete, Meso-mechanics, Finite element method, Interface elements.

Abstract. This paper describes recent numerical simulation results of a purely mechanical study of the effects of high temperature in mortar and concrete. The material has been considered as a two-phase composite, with different thermal expansion laws of matrix and particles taken from the literature. The numerical simulation is based on a meso-mechanical model developed in the group of Mechanics of Materials UPC, which represents the largest aggregate particles explicitly, and represent cracks in a discrete manner by inserting zero-thickness interface elements in all potential crack trajectories a priori of the analysis. The differential expansions create tensile stresses and therefore cracking, that eventually may close, reopen and lead to non-trivial overall material behavior. The results are discussed and compared to the experimental information available, and lead to a general good agreement, capturing the essential mechanisms described in the literature.

1 INTRODUCTION

Under high temperature variations, heterogeneous materials such as concrete may develop internal stresses and complex behavior including cracking and degradation as the result of the expansion mismatch between components. Cruz and Gillen [1] show experimental results of thermal expansion of concrete specimens, as well as of individual ingredients: cement paste, mortar and dolomite rock. In their tests, temperature ranged between 27 and 871ºC. The experimental test was carried out on cylindrical samples of 13mm in diameter and 76 mm in length. Experimental results show a variable coefficient of thermal expansion for cement paste, first expanding (until approximate 180ºC) and then contracting. In contrast, Dolomite rock shows, between 93 and 871ºC, an almost linear expansion as temperature is increased. Figure 1 shows the experimental results that were taken as the basic input information for the numerical study of Sect. 3.1, which deals with the free expansion of mortar specimens. Additional results also reported in the paper, deal with the influence of pre-imposed vertical stresses or prescribed deformations on the expanding specimen, as reported from Anderberg and Thelandersson [2], Thelandersson [3] and Willam et al. [4].

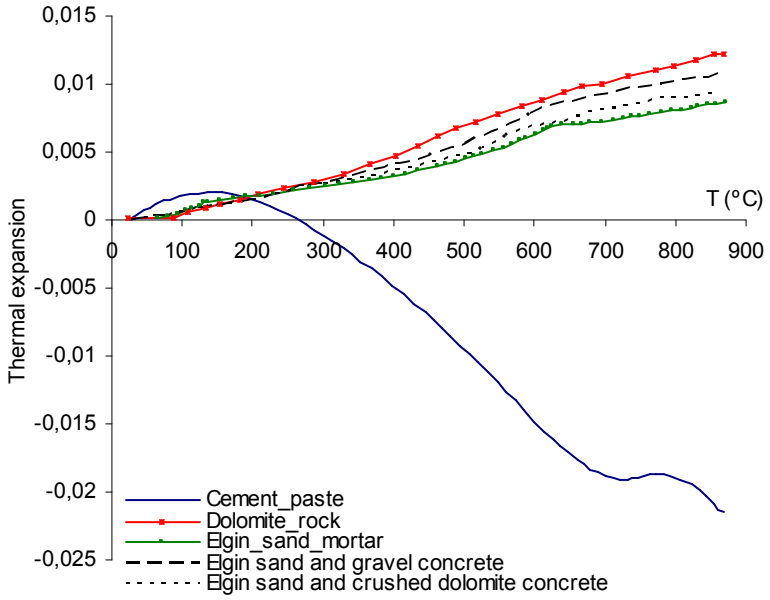

Figure 1: Experimental results for cement paste, dolomite rock, mortar and concrete (from Cruz and Gillen [1]).

2 MESOMECHANICAL MODEL

The numerical simulation is based on a meso-structural model in which the largest aggregate particles are represented explicitly, surrounded by a homogeneous matrix representing the average behavior of mortar plus the smaller aggregates. In order to capture the main potential crack trajectories, zero-thickness interface elements are inserted *a priori* of the analysis, along all the aggregate-mortar and some of the mortar-mortar mesh lines. These interface elements are equipped with a nonlinear constitutive law based on elasto-plasticity and concepts of fracture mechanics, which is formulated in terms of normal and shear components of the stress on the interface plane and the corresponding relative displacement variables. The initial loading (failure) surface F = 0 is given as three-parameters hyperbola (tensile strength χ, asymptotic cohesion c and asymptotic friction angle tanϕ). The evolution of F (hardening-softening laws), is based on the internal variable W^{cr} (work spent in fracture processes), with the two material parameters G_F^I and G_F^{IIa} that represent the classical fracture energy in Mode I, plus a second fracture energy for an "asymptotic" Mode IIa under shear and high confinement. A more detailed description of this elasto-plastic constitutive law can be found in the literature [5,6]. Results of the meso-mechanical model for normal concrete specimens subject to a variety of loading cases in 2D and 3D can also be found elsewhere [6-9].

For the current study, some of the FE meshes used previously have been modified in the sense of adding some interface elements along mesh lines perpendicular to the aggregate surfaces at mid-distance between aggregate corners. In this way, the medium surrounding the expanding aggregate particle can crack in the direction that is more physical, and possible spurious tensile stresses in the surrounding material are minimized.

3 RESULTS AND DISCUSSION

3.1 Thermal expansion of mortar specimens

The first numerical analysis is a mortar specimens composed by small aggregate particles of dolomite embedded in a cement paste matrix. For the cement paste the expansion vs. temperature law is extracted directly from the experimental curve above (in figure 1). Since the curve shows first expansion and then contraction, the thermal coefficient, which corresponds to the secant line from the origin to the desired point on the curve, changes sign from positive to negative as temperature increases. For dolomite rock, which constitutes the sand, experimental results show an almost linear expansion as temperature is increased. For this reason a constant coefficient of thermal expansion has been used in the calculations, with a value of 0.0000125/ºC.

In the experiment, thermal expansions were also measured for the overall mortar specimens, these values have been used to compare the results from the numerical calculations. For the numerical simulation, a 12x12 mm^2 square specimen was considered with volume fraction of sand aggregates 39% and maximum size 1.7mm (average aggregates size 1.02mm). These values were adopted based on available data from the lab specimens. The resulting meso-geometry and FE mesh are shown in figure 4.

3.1.1 Elastic analysis

The first analysis run for the mortar specimen has been under the assumption of linear-elastic interfaces (figure 2). Note that in this case interfaces are not allowed to open (crack) or slide. Therefore, the change from expansion to contraction of the cement paste for high temperature, forces the overall initial mortar expansion (with tensioned sand aggregates) to turn later into overall contraction (with compressed sand aggregates), and all materials and interface are assumed to withstand tensile stresses without limit.

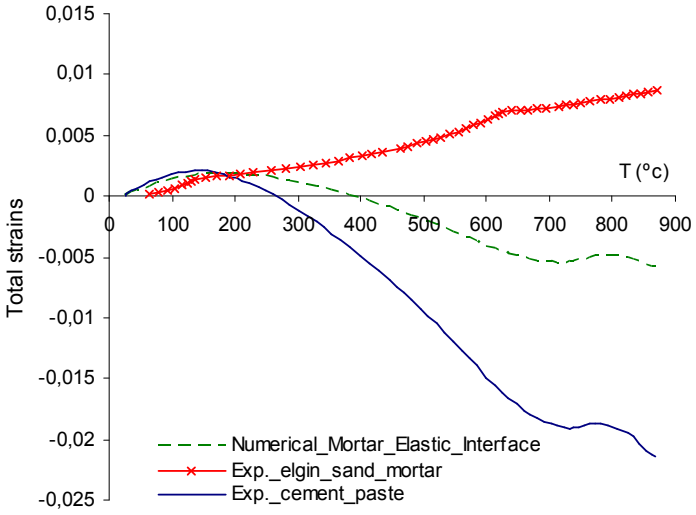

Figure 2: Experimental curves for mortar and cement paste expansion, together with numerical results of a heterogeneous mortar specimen assuming linear elasticity (linear elastic interfaces).

3.1.2 Non-linear analysis with cracking

In this case the interface elements are assumed to follow a fracture-based non-linear constitutive law with softening that simulates cracking [5]. The material parameters used are: for the continuum medium: E = 70000 MPa (dolomite rock), E = 25000 MPa (cement paste) and υ = 0.2 (both); for all interfaces (along both dolomite sand-cement and cement-cement contacts): $K_N = K_T$ = 500000 MPa/mm, $\tan\phi_0$ = 0.90, χ_0 =6 MPa, c_0 = 15MPa, G^F_I = 0.025 N·mm, $G^F_{II} = 10\ G^F_I$, σ_{dil} = 40 MPa, α_d = -2.

Figure 3 shows the numerical and experimental results obtained for mortar specimens, together with the experimental results for dolomite rock and cement paste.

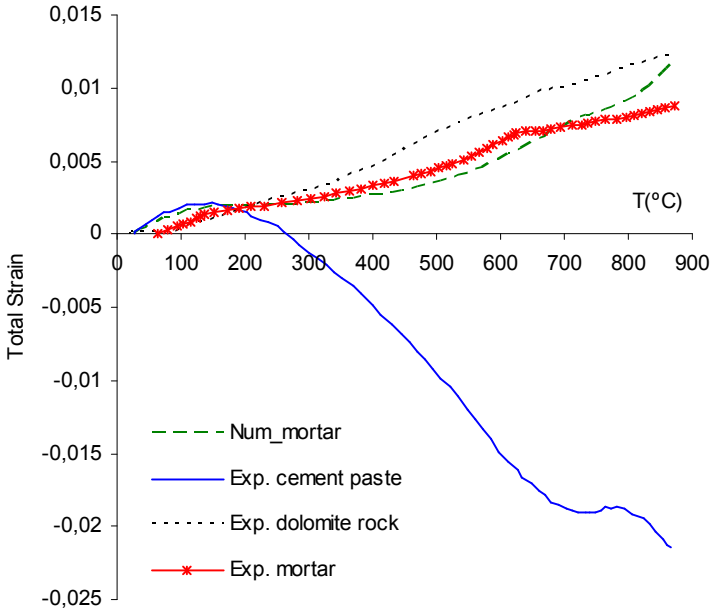

Figure 3: Numerical versus experimental specimen expansion curves for the mortar specimen with cracking, together with the curves obtained for sand and for cement paste.

3.1.3 Crack evolution and final deformation

Figures 4 and 5 show the details of crack evolution for eleven different prescribed temperature values (54, 110, 148, 180, 192, 286, 547, 612, 711, 806 and 867ºC), as well as the final deformation mesh (in the last diagram for 867 ºC, the red mesh overlapped represents the undeformed mesh). In the figures, cracking is represented in term of the magnitude of the relative displacement vector (square root of normal plus tangential relative displacements squared). The graphic scale factor is not the same in all figures because for temperatures below 201ºC displacement magnitudes are significantly lower than for temperatures above that value. The maximum values of the relative displacement norm obtained through the entire mesh for each temperature are indicated in the figure captions.

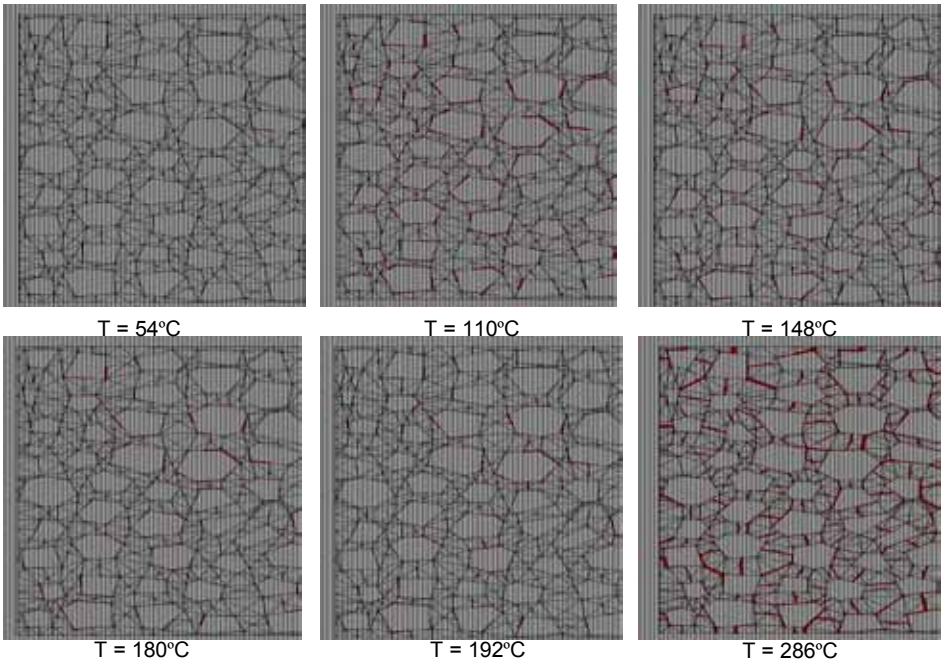

Figure 4: Crack pattern evolution of mortar in terms of the magnitude of the relative displacement vector, for increasing prescribed temperature (same graphic scale factor for the six diagrams, but not the same as in figure 5; maximum value for each diagram (x10-4): 0.131, 0.204, 0.193, 0.169, 0.158 and 4.24).

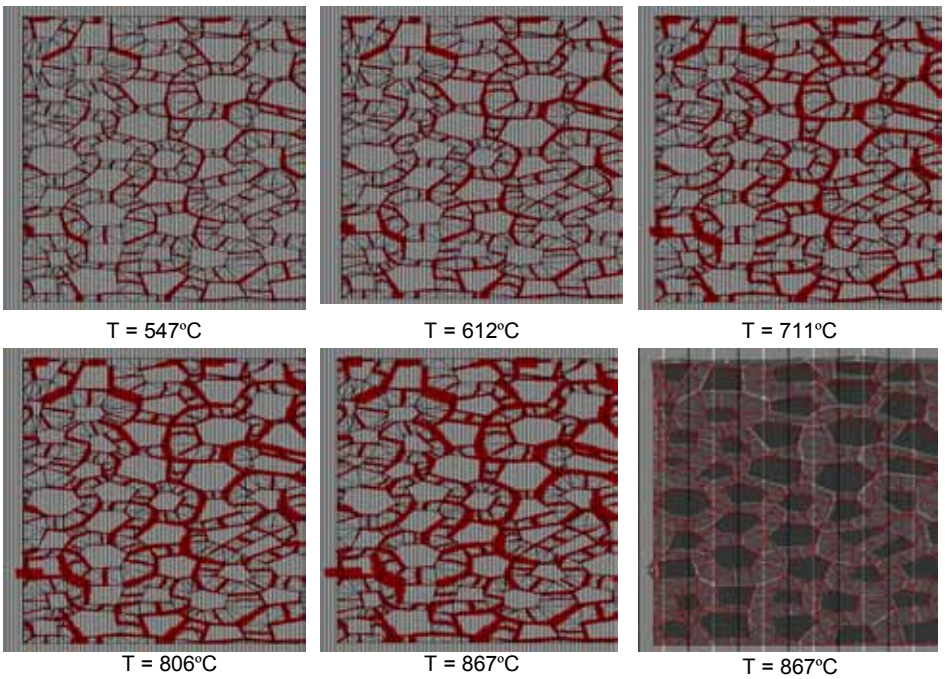

Figure 5: Crack pattern evolution of mortar in terms of the magnitude of the relative displacement vector, for increasing prescribed temperature (same graphic scale factor for the five diagrams, but not the same as in figure 4; maximum value for each diagram(x10-4): 33.9, 46.1, 60.3, 65.1 and 78.8).

In figures 4 and 5 it is shown that initially only the interface elements between aggregate and matrix develop cracks (three first pictures in figure 4), while for higher temperature practically all interface elements become activated. This is related to the fact that for temperature below 180ºC the aggregates are basically in tension and the matrix is in compression, while for higher temperature this situation is inverted.

3.1.4 Evolution of the stresses of the continuous medium

Figure 6 shows the evolution of the stresses within the cement paste and sand grains (continuous medium), red color representing tensile stresses and blue color compressive stresses. For temperatures below 180ºC, cement paste expands more that the aggregates (see figure 1), causing the aggregates to be subject to tension and the matrix to compression. Above that temperature, however, this trend is inverted: the aggregates expand more that the cement paste and the stresses change sign. In figure 6 we can see both states:

- Below 180ºC the aggregates are in tension and the matrix is in compression. Stress values increase until 110ºC, then start decreasing.
- Above 180ºC the stress state changes and aggregates turn into compression while the matrix turns into tension. Once signs have changed, stress values increase until approximately 286ºC, and beyond that temperature they decrease again.

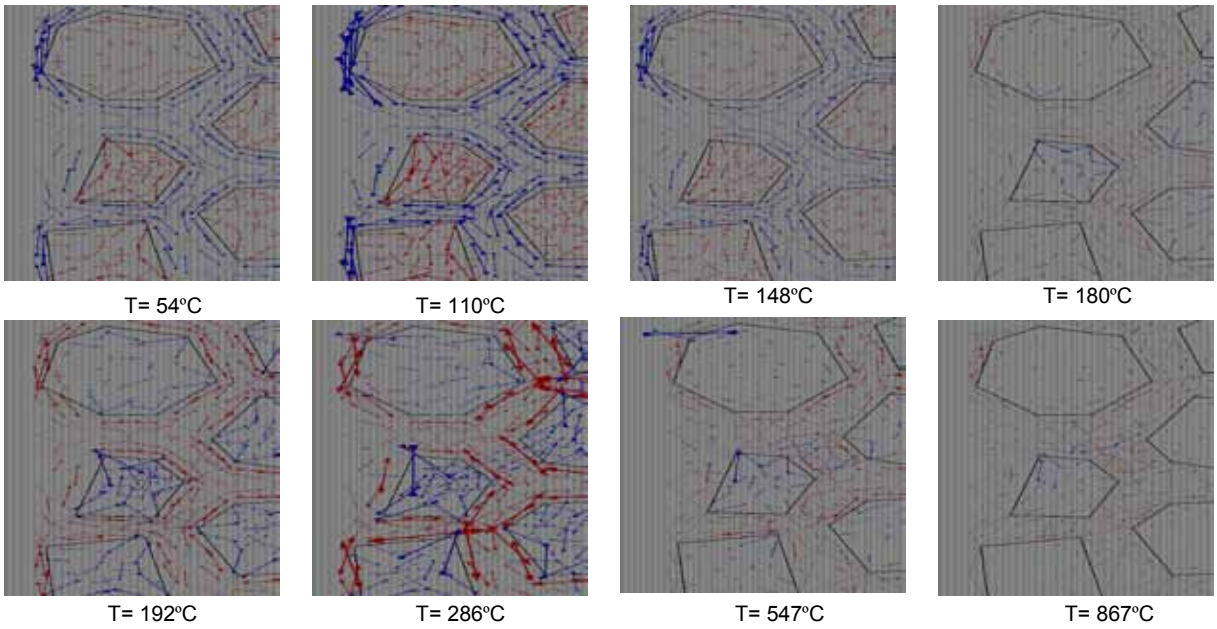

Figure 6: Evolution of stresses in the continuous medium of aggregates and matrix for the following temperature values: T = 54ºC, 110ºC, 148ºC, 180ºC, 192ºC, 286ºC, 547ºC and 867ºC, same scale factor for stresses in all graphs in this figure.

3.1.5 Numerical estimate of the influence of pre-existing vertical compressive stress

The fact that thermal action without confinement generates cracking, motivates the investigation of the effects of simultaneous loading and temperatures. Intuitive understanding tells us that under initial compression, cracking caused by tensile stress increments generated by temperature action might be postponed or prevented altogether. Therefore the combined effects of compression and temperatures might differ significantly from the superposition of the individual effects. These aspects are investigated in this section, by means of some additional calculations, using the same mortar mesh of the previous section with the parameters already calibrated for the mortar of Cruz and Guillen [1], which is subject to simultaneous thermal action and vertical confining stress. Because Cruz and Guillen [1] did not perform any such test under compressive load, the numerical results obtained are compared in a pure qualitative manner with some existing experimental results of Anderberg and Thelandersson [2], which were carried out in concrete specimens with different properties and geometric characteristic of the mortar used in the simulation.

In the numerical simulations, the specimens were loaded to a certain vertical stress level and then heated to 800ºC. The load level is given as a percentage of the compressive strength of the material. Ten specific cases were analyzed with the nine compressive vertical stresses over f'_c values of: 0, 0.01, 0.03, 0.05, 0.112, 0.225, 0.450, 0.675 and 1. The results obtained in terms of overall vertical strain (positive = expansion, negative = contraction) against temperature are shown in figure 7.

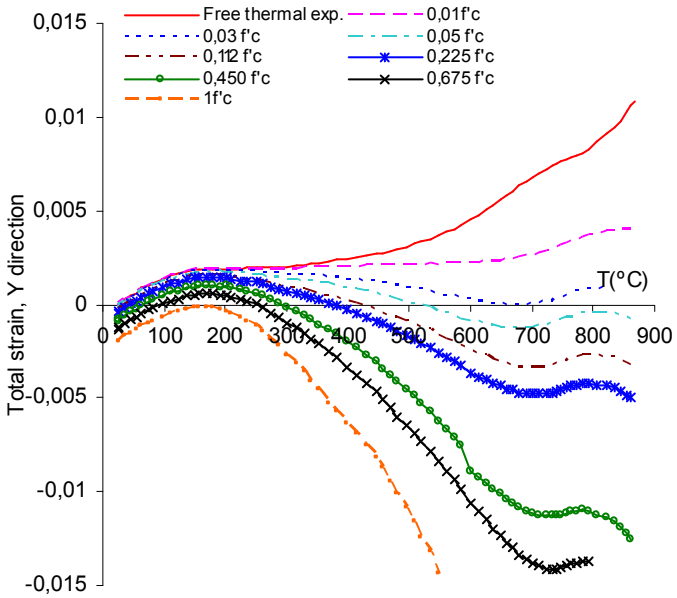

Figure 7: Total strain vs. temperature for different stress levels (numerical study).

In the figure, the upper continuous curve corresponds to free expansion (no compression), and coincides with the mortar curve in figure 3. For low temperatures, the effect of compression on the thermal expansion is reflected by the shift downwards of each curve,

which remains approximately constant until the temperature of 200-300^{0}C. In this range the effects of compression and temperatures could be simply superimposed. Beyond that temperature, however, the (upper) uncompressed curve shows an inflection point corresponding to the beginning of internal cracking when the contracting matrix gets detached from the expanding aggregates, while the pre-compressed curves tend to turn downwards following the matrix contraction. Tensile stresses due to thermal mismatch have to overcome existing compressions, with the result that cracking and overall expansions are delayed to higher and higher temperatures, or even suppressed altogether for high compression values approaching the compressive strength.

The main trends observed in the computations are similar qualitatively to those observed in the experiments A5, A6, A8 and A9 of Anderberg and Thelandersson [2], results that are shown in section 3.2.2 (figure 10).

3.2 Thermal expansion of concrete specimens

Experimental tests of thermal expansion at high temperature of concrete specimens with and without compression stress were reported, among others, by Anderberg and Thelandersson [2]. The calculations in this section try to reproduce those material characteristics and results, but due to the lack of basic material information (those authors did not report details of thermal expansions of the individual components cement, aggregate, mortar), the missing information is taken from the experiments from Cruz and Guillen [1] already mentioned in previous sections.

In the numerical analysis, concrete is represented by large aggregates particles of dolomite rock surrounded by a matrix that represents mortar and smaller aggregates. The specimen considered has dimensions 10x10cm^2, volume fraction of large aggregates 28% and maximum aggregate size 14mm (average aggregate size 10.4mm). The material parameters are: E = 70000 MPa (dolomite rock), E = 29000 MPa (mortar) and υ = 0.2 (both); for dolomite aggregate-mortar interfaces $K_N = K_T$ = 500000 MPa/mm, $tan\phi_0$ = 0.90, χ_0 =4 MPa, c_0 = 15MPa, G^F_I = 0.025 N·mm, G^F_{II} = 10 G^F_I, σ_{dil} = 40 MPa, α_d = -2, and for mortar-mortar interfaces: $K_N = K_T$ = 500000 MPa/mm, $tan\phi_0$ = 0.90, χ_0 =6 MPa, c_0 = 20MPa, G^F_I = 0.030 N·mm, G^F_{II} = 10 G^F_I, σ_{dil} = 40 MPa, α_d = -2.

3.2.1 Free thermal expansion analysis

In the numerical simulation of the free thermal expansion analysis of concrete, the variable coefficient of thermal expansion for mortar is extracted from a volume expansion vs. temperature curve obtained numerically in Sec. 3.1.2 (figure 3). For aggregates, the coefficient of thermal expansion is assumed constant with value 0.0000125/ºC (same as for the sand in the mortar simulation of Sect 3.1).

Figure 8 shows the numerical and experimental results for concrete specimens, for both Cruz and Guillen [1] and Anderberg and Thelandersson [2]. Numerical results are closer to the curves reported by Cruz y Guillen [1], and do not deviate excessively from those by Anderberg y Thelandersson [2] either. Results also show that in general terms expansion of concrete is larger than of mortar subject to the same temperature.

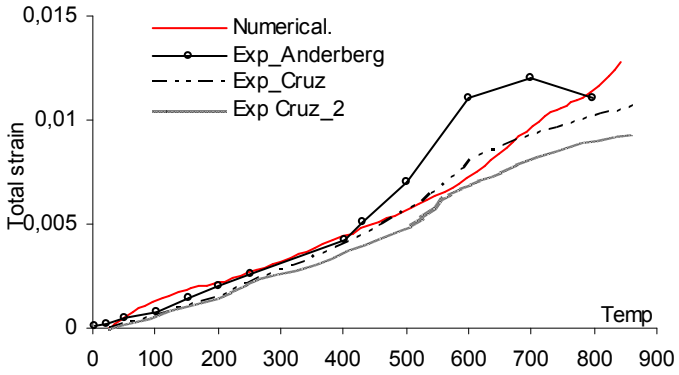

Figure 8: Total strain vs. temperature, numerical and experimental results for concrete.

3.2.2 Crack evolution and final deformation

The crack evolution trend is similar to that obtained for mortar in section 3.1.3. Figure 9 shows a detail of crack evolution for three different prescribed temperature values (157, 519 and 867ºC) and the final deformation field. We can see that, as in mortar, initially only the interface elements between aggregate and matrix are opening, while for higher temperature practically all interface elements became activated.

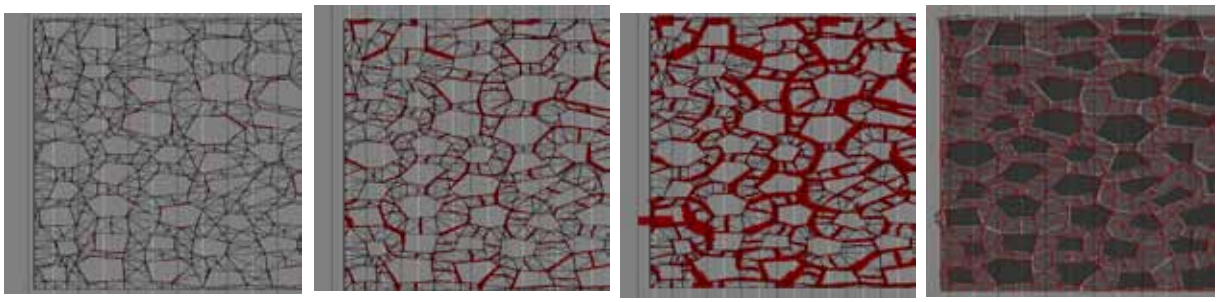

Figure 9: Crack pattern evolution of concrete in terms of the magnitude of the interface relative displacements, for increasing prescribed temperature. Max. values obtained through the mesh (x10-3): 0.1766, 5.096, and 5.970, respectively.

3.2.3 Test with thermal action under different values of vertical compressive stress

The influence of a pre-existing sustained vertical stress on the evolution of thermal expansion is analyzed. The specimens were loaded to a certain vertical stress level and then heated to 800ºC. The load level is given as a percentage of the compressive strength of the material. Three specific cases were analyzed with the three compressive vertical stresses over f'_c values of: 0.225, 0.450 and 0.675. For each cases here analyzed a constant coefficient of thermal expansion of value 0.0000125/ºC for the aggregates was used. For the mortar, a variable thermal coefficient has been extracted from the mortar expansion/contraction curves obtained in Sect. 3.1.5.

Figure 10 shows preliminary numerical results obtained in terms of overall vertical strain (positive = expansion, negative = contraction) against temperature, together with the experimental curves of Anderberg and Thelandersson [2]. For low temperature values, approximately 0-300ºC, there is a certain difference between numerical and experimental result, this is due to the fact that the experimental curves show for this range of temperatures the called transitional thermal creep which our model is not able to capture. For higher temperature values, where cracking and overall expansion are delayed for the presence of the vertical compressive stress, there is a qualitatively good agreement between results.

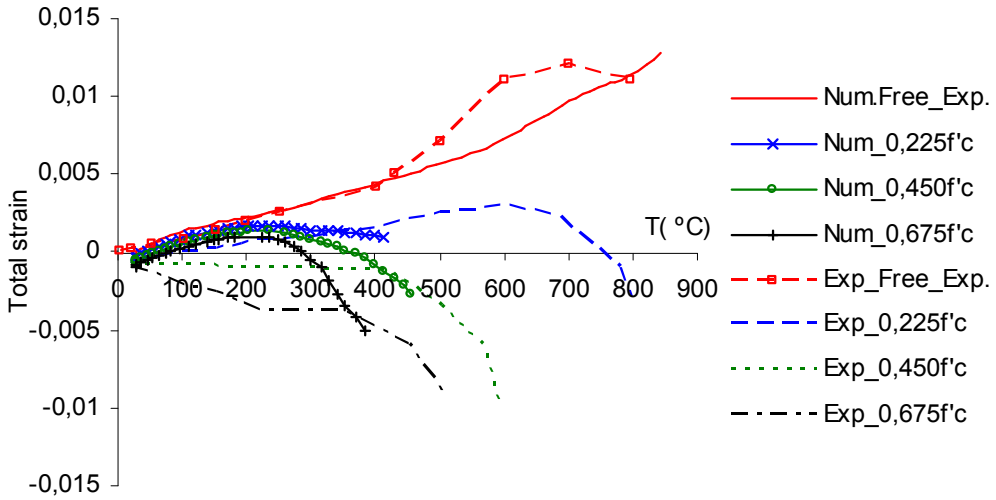

Figure 10: Total strain vs. temperature for numerical and experimental curves [2] for different load levels.

Figure 11 depicts the evolution of microcracking with increasing temperature, in the analysis under a vertical pre-compression level of $0.450f'_c$, as well as the final deformed mesh. The representation is made in terms of the magnitude of the interface relative displacements. It can be observed as cracks develop predominantly in the vertical direction, with slight lateral inclination. This is in contrast with the circumferential-radial crack patterns around aggregates observed in the case of free expansion with no vertical compression (figure 9).

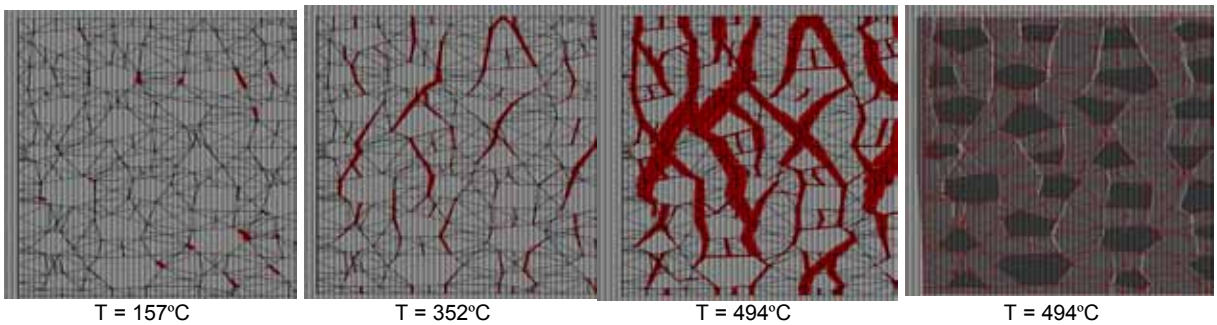

Figure 11: Crack pattern evolution in concrete in terms of magnitude of interface relative displacements, for increasing prescribed temperatures with a pre-compression stress level of $0.450f'_c$, and final deformed mesh. Max. values obtained for each diagram (x10-3): 0.020, 9.04 and 336.

4 CONCLUDING REMARKS

The purely mechanical approach employed, which is based on input data of expansion curves for individual components, plus a meso-mechanical model with interfaces for cracking, seems capable of representing the effects of temperature mismatch on the overall expansion of mortar and concrete specimens, and related degradation mechanisms of cracking and damage. On-going work is aimed at improving the material model under loading by incorporating transitional creep at high temperatures, reproducing additional results of displacement-restrained experiments, and incorporating into the model additional capabilities for temperature distribution and other diffusion-related phenomena linked to high-temperatures.

ACKNOWLEDGEMENTS

This research has been supported partially by research projects BIA2009-10491 funded by MICINN (Spain), and 2009SGR-180 from AGAUR-Generalitat de Catalunya (Barcelona). The first author is grateful to MEC, Madrid, for her FPI doctoral fellowship.

REFERENCES

[1] Cruz, C. R., and Gillen, M. Thermal expansion of Portland cement paste, mortar and concrete at high temperatures. *Fire and materials,* vol.4 nº2, pp. 66-70 (1980).
[2] Anderberg, Y., and Thelandersson, J. Stress and deformation characteristics of concrete at high temperatures. *Technical Report, Lund Institute of Technology,* Lund, Sweden (1976).
[3] Thelandersson, S. Modeling of combined thermal and mechanical action in concrete. *J. Engrg. Mech.,* ASCE 113(6), pp. 892-906, (1987).
[4] Willam, K., Rhee, I., and Shing, B. Interface damage model for thermomechanical degradation of heterogeneous materials. *Comp. Methods Appl. Mech. Engrg*. 193, pp. 3327-3350, (2004).
[5] Carol, I., Prat, P. C., López, C.M. *J.* A normal/shear cracking model. Application to discrete crack analysis. *Engng. Mech. ASCE*, 123, pp. 765–773 (1997).
[6] Carol, I., López, C.M. and Roa, O. Micromechanical analysis of quasi-brittle materials using fracture-based interface elements. *Int. J. Num. Meth. Engng.*, Vol 52, pag. 193-215 (2001).
[7] López C.M., Carol I., Aguado A. Meso-structural study of concrete fracture using interface elements. I: numerical model and tensile behaviour. *Materials and Structures*, Vol. 41, Nº 3, pag. 583-599 (2008).
[8] López C.M., Carol I., Aguado A. Meso-structural study of concrete fracture using interface element II: compression, biaxial and Brazilian test. *Materials and Structures*, Vol. 41, Nº 3, pag. 601-620 (2008).
[9] Caballero, A., Carol, I., López C. M. 3D mesomechanical analysis of concrete specimens under biaxial loading . *Fatigue and Fracture Engng. Mat. and Structures*, 30, 877-886 (2007).